Eur. Phys. J. B **16**, 295–301 (2000)

THE EUROPEAN PHYSICAL JOURNAL B

EDP Sciences

Electromodulated infrared transmission spectra of blue bronze

B.M. Emerling, M.E. Itkis, and J.W. Brill[a]

Department of Physics and Astronomy, University of Kentucky, Lexington, KY 40506-0055, USA

Received 21 February 2000

Abstract. The infrared transmission of the quasi-one dimensional charge-density-wave (CDW) conductor blue bronze ($K_{0.3}MoO_3$) is affected by polarization of the CDW, and therefore by application of a voltage near or above the threshold for CDW depinning. In this paper, we compare the spectra associated with the relative change in transmission ($\Delta\tau/\tau$) taken for different temperatures and oscillating voltages. We find that the phonon spectrum is affected by CDW polarization; the linewidths or frequencies of most phonons change by ≈ 0.01 cm^{-1}. However, no new intragap states that can be associated with current injection are observed; *i.e.* the spectra associated with polarization of the CDW in the crystal bulk is identical to that associated with CDW current injection near the contacts. Our results indicate that, for light polarized perpendicular to the conducting chains, the density (n), cross-section (σ), and bandwidth (Γ) of intragap states are related by: $n\,\sigma/\Gamma < 10^{-10}$ (Å cm^{-1})$^{-1}$. For expected values of the cross-section and bandwidth, this implies that the intragap states can be optically excited for a time less than 0.3 μs.

PACS. 71.45.Lr Charge-density-wave systems – 78.20.Jq Electrooptical effects – 72.15.Nj Collective modes (e.g., in one-dimensional conductors)

1 Introduction

Quasi-one-dimensional conductors with sliding charge-density waves (CDW's) exhibit some of the most unusual phenomena of any solids, many of which result from the ease with which the CDW is deformed. In zero field, the CDW deforms to accommodate impurities. Small applied voltages cause the CDW to strain from this configuration, giving rise to very large ($> 10^8$) dielectric constants. When the voltage exceeds a threshold V_T, the CDW slides through the crystal, carrying current [1].

A long-standing question has concerned the mechanism of current conversion at the contacts when the CDW is sliding. Current conversion requires removing (adding) wavefronts at the positive (negative) current contact. These phase-slip processes can be viewed as the growth of CDW "dislocation loops", surrounding chains in which the phase has changed by 2π (corresponding to two electrons), and are believed to be driven by longitudinal strains in the CDW [2–6]. Recently, these strains have been "imaged" using multicontact transport measurements [7,8], X-ray diffraction [9], and a novel electrooptic technique [10,11], the subject of this paper.

The actual formation of the dislocation loops, however, is poorly understood. It is thought that when an electron enters a CDW chain, it forms a "π-soliton" state with energy near the center of the CDW gap. These are expected to quickly (≈ 1 ps) pair into 2π-solitons, with energy levels near the edge of the gap [12]. It is not known how quickly these coalesce into dislocation lines and whether their energies remain well-defined near the gap edge, or whether they oscillate through the gap [13].

We recently observed that the infrared transmission (τ) of $K_{0.3}MoO_3$ ("blue bronze"), a quasi-one-dimensional metal which undergoes a phase transition into a semiconducting CDW state at $T_c = 180$ K [14], is affected by the application of an electric field [15]. For ≈ 5 μm thick samples, τ increases (decreases) by $\approx 1\%$ near its positive (negative) contacts, respectively. This electrooptic effect occurs for voltages $V > V_P$, the voltage at which one first observes CDW polarization, and we associated the change in transmission with the CDW strain [15]. (V_P is less than V_T, the threshold for sliding, as discussed below.)

For $T < 100$ K, the relative change in transmission, $\Delta\tau/\tau$, is activated [15], suggesting that it is due to changes in the density of thermally excited quasiparticles, n_{qp}, screening the CDW strain. Furthermore, the spectra of $\Delta\tau$ and τ are similar [15,16]; since $\Delta\tau/\tau$ is approximately proportional to the change in absorptivity (see below), this implies that a broadband absorption process is involved in this electrooptic effect, in contrast to effects observed at critical points in the bandstructures of conventional semiconductors [17]. In blue bronze, the mobile quasiparticles are negative [18]. Since the applied field will cause the negative CDW to compress at the positive current contact, the negative quasiparticles will accumulate at the negative contact, which will increase their intraband absorption there, consistent with the sign we observe. Assuming that intraband absorption is the only process

[a] e-mail: jwbrill@pop.uky.edu

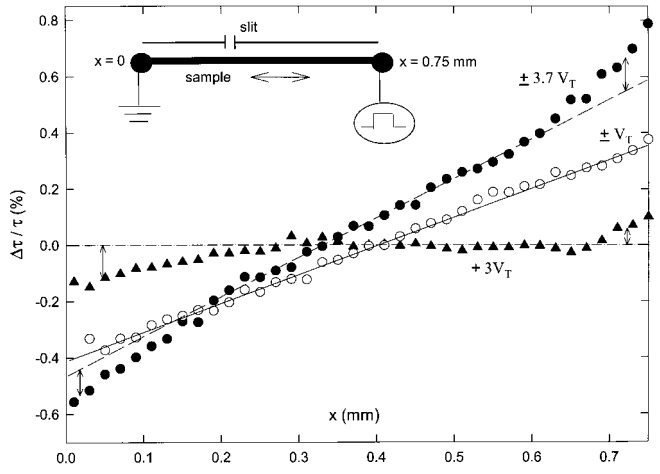

Fig. 1. Spatial dependence of $\Delta\tau/\tau$ (adapted from Ref. [11]) as measured with bipolar square waves at $\pm 3.7\,V_{\rm T}$ and $\pm V_{\rm T}$, and with a unipolar square wave, $+3\,V_{\rm T}$. The lines through the points show the $\Delta\tau/\tau$ variations associated with bulk polarization of the CDW, and the vertical arrows (for $\pm 3.7\,V_{\rm T}$ and $+3\,V_{\rm T}$) indicate representative contact contributions. The inset shows the experimental set-up.

affected by the field, we estimated that the change in $n_{\rm qp}$ at the contacts, expected to be proportional to the gradient of the CDW phase ($\partial\phi/\partial x$) [6], was close to 100% for $V \approx V_{\rm T}$ [15].

We measured the spatial distribution of $\Delta\tau/\tau$ by moving the sample behind a narrow (30 μm) slit, as shown in the inset to Figure 1 [10,11]. A square wave voltage was applied to the sample, allowing measurement of $\Delta\tau$ with a lock-in amplifier. Representative $\Delta\tau/\tau$ "images", taken with symmetric bipolar square waves ($\pm V$), for which the measured signal is proportional to the difference in transmission when the voltage is positive and negative, and with a unipolar square wave, for which the signal is proportional to the difference in transmission between positive applied voltage and zero, are shown in Figure 1 [11].

For bipolar voltages $> V_{\rm T}$, the spatial distribution of $\Delta\tau/\tau$ is remarkably similar to that of $\partial\phi/\partial x$ determined for another CDW conductor, $NbSe_3$, by X-ray diffraction [9] and transport measurements [7,8], further justifying the approximation $\Delta\tau/\tau \propto \partial\phi/\partial x$; this similarity is especially surprising because $NbSe_3$ remains semimetallic, with a large density of quasiparticles, in its CDW state [19]. In the bulk of the sample, $\Delta\tau/\tau$ varies linearly with position, and is zero near the center of the sample. However, the change in transmission exceeds the extrapolated bulk value near (≈ 100 μm) the current contacts; this extra contact strain, represented by vertical arrows in the figure, is associated with the extra strains $\partial\phi/\partial x$ needed to drive phase-slip and current conversion [7,8,10].

It has been suggested, based on consideration of the strain profiles observed in $NbSe_3$, that the bulk deformation occurs only if the quasiparticle and collective currents fail to equilibrate, *e.g.* due to the finite contact separation or pinning of dislocations [6,9]. However, our blue bronze samples differ in an important way from the $NbSe_3$ samples: for our samples, considerable bulk deformations are observed even for voltages at which there is no steady CDW current, *i.e.* for $V_{\rm P} < |V| \leq V_{\rm T}$. This difference is presumably because the CDW is more strongly pinned at the contacts than in the bulk in our samples. As mentioned above, $V_{\rm P}$ is the lowest voltage for which changes in the bulk polarization, observed through the "overshoot effect" [15,20], are observed. Figure 1 shows the spatial variation of $\Delta\tau/\tau$ measured for the bipolar square wave $V = \pm V_{\rm T}$; there is a large linear variation throughout the sample, reflecting the bulk polarization, but no extra contact deformation (*i.e.* no current conversion) [10]. The bulk deformation is pinned in place if the applied field is removed (rather than reversed); this is the "remanent polarization" effect [20]. For example, Figure 1 also shows data taken with a unipolar square wave ($V = +3V_{\rm T}$) [11]. Because the bulk deformation does not change, it does not give rise to an oscillating signal, so only the signal from the contact deformation is measured with the lock-in amplifier.

In subsequent work, we measured portions of the electromodulated transmission spectrum using a broadband source and grating monochromator [16]. We found that the spectrum of $\Delta\tau$ is in fact not identical to that of τ, and that phonon absorption lines were affected by the CDW deformation. In the spectral region investigated, the voltage dependent changes in τ were similar to changes in transmission observed when changing temperature. However, that investigation was limited by the low spectral intensity of the light. In particular, we could not investigate the electromodulated spectrum where the absorption is strong (*i.e.* near the centers of strong phonon lines and along the edge of the CDW gap), and we could not measure spectra associated with the spatially confined contact deformations at all.

In this paper, we report on new measurements of the electromodulated transmission spectra, made using tunable lead salt diode lasers [21]. The major motivation for this study was to search for new intragap excitations that could be associated with soliton states needed for current conversion near the contacts [12]. To identify these, we compared the electromodulated spectrum associated with the contact strain with that coming from the bulk polarization. While no new excitations were observed in the contact spectrum, we did observe that phonons were affected by the CDW polarization in unanticipated ways. We studied the temperature dependence of the spectra to try to understand these CDW-phonon interactions. Brief reports of some of these results were published in references [22,23].

2 Experimental details

Samples were prepared by using sticky tape to cleave as-grown crystals to thicknesses ranging from 3 to 10 μm. After cleaving, crystals were typically 1 mm long (in the high conductivity direction) and 0.5 mm wide. Samples were then etched in dilute NH_4OH. Copper films were

evaporated on the ends of the crystals for current contacts, and the samples were mounted with silver paint on substrates. Because these thin samples are extremely fragile, only one end of the sample was attached directly (*i.e.* heat sunk) to the substrate with the silver paint; the other end was attached with a thin silver wire. The substrates were glued to the cold finger of an optical cryostat, and two-probe measurements were used to monitor the sample's I-V characteristics [1,14].

Two different types of substrates were used. For two of the samples discussed below, we used thin KRS5 disks onto which opaque films were evaporated. The sample was mounted with its fixed contact adjacent to a slit in the film. For sample A, the slit width was 160 μm, while for sample C it was 400 μm. KRS5 substrates have the advantage of being transparent in the mid-IR, but they have the disadvantage that their thermal expansivity differs considerably from that of blue bronze, increasing the probability of the sample breaking when changing temperature. Sample B was instead mounted on a silicon substrate, which better matches the thermal expansivity of blue bronze. The "slit" was made by etching a 250 μm hole in the silicon, which was coated with an opaque film.

We used four tunable diode lasers [21], cooled with a closed-cycle helium refrigerator, as light sources. The four lasers cover the range 400-1 300 cm^{-1} with typical powers 1/4 mW. The light was focused onto the slit in the substrate with a 6:1 off-axis ellipsoidal mirror, and then refocused onto a Ge(Zn) photodetector. Since the samples will transmit light primarily polarized perpendicular to the conducting chains, the incident light was polarized in this direction to reduce sample heating, which was always less than 0.01 K. To increase the signal, the lasers were not mode selected. The number of modes excited, and therefore the bandwidth of the signal, varied with laser tuning (*i.e.* temperature), but typically there were a few modes spread over < 14 cm^{-1} (see Fig. 2 below).

Measurements were made by exciting the sample with a square-wave voltage, and two lock-in amplifiers were used to simultaneously measure the detector signals at the square-wave (f) and chopping (F) frequencies. The ratio of these signals, $V(f)/V(F) = \Delta\tau/\tau$. For unipolar square-waves, the frequency ($f = 320$ Hz) was much greater than the thermal relaxation rate, so that Joule heating caused a negligible signal. When the sample was removed from the substrate, the spectral intensity of light transmitted through the slit was measured to determine $\tau(\nu)$. (It was important to use a similar aperture for the normalization, because the spatial distribution of the focused light varied with laser frequency.)

Since $\Delta\tau/\tau$ varies strongly with position in the sample, as shown in Figure 1, it will also be affected by the transverse mode structure of the laser light. Typically, the lasers were focused to a spot of average diameter ≈ 1 mm, but spatial variations with a length scale ≈ 0.2 mm occurred within this spot. These variations changed gradually with laser tuning, so they could affect $\Delta\tau/\tau$ values measured at very different frequencies (*e.g.* > 100 cm^{-1}) or with different lasers, especially for sample C, which had the largest aperture. Furthermore, because of vibrations from the laser's refrigerator, the spatial structure in the focused light created "noise" roughly proportional to the electromodulated signal. Therefore, as compared to our previous measurements with a broadband source, the present studies have much greater sensitivity to weak signals but increased overall noise.

Assuming near normal incidence and neglecting multiple internal reflections, the transmission is given by $\tau \approx (1-R)^2 \exp(-\alpha d)$, where d is the thickness, α the absorptivity, and R the reflectivity [16], so that $\Delta\tau/\tau \approx -d\Delta\alpha - 2\Delta R/(1-R)$. (For our samples, $\alpha d \approx 1$ at energies where the absorption is weak [16].) Sample dependence of $\Delta\tau/\tau$ spectra may therefore also be due to different sample thicknesses. However, simulations show that α and R are affected similarly by changes in the strength, frequency, or width of absorption lines, and so will cause similar line shape changes in the $\Delta\tau/\tau$ spectrum.

3 Comparison of bulk and contact electromodulated spectra

Figure 2 shows $\Delta\tau/\tau$ spectra for sample A at $T = 81$ K taken with each of the 4 lasers. Also shown for reference is the optical density of the sample, $-\ln(\tau)$ and error bars representing the typical spectral resolution (reflecting the multimode operation of the lasers) and scatter in $\Delta\tau/\tau$. The optical density spectrum is similar to that of the transverse conductivity (determined from the reflectivity), with prominent phonon absorption lines (labeled A-J in Figs. 2a, b, c) at the same energies [24–26]. Figure 2d shows the absorption edge associated with the CDW energy gap.

Electromodulated spectra were measured using both a bipolar square-wave voltage ($V = \pm V_{\rm T}$) and a unipolar square-wave voltage ($V = 3.2V_{\rm T}$). As discussed above, the former is only sensitive to the bulk deformation, while the latter is only sensitive to the contact deformation. The contact signal is multiplied by $N = 2.45$ to facilitate comparison of the two spectra. As mentioned above, current conversion is expected to involve long-lived 2π-soliton states, with energy levels in the gap, within $\approx kT_{\rm c} = 125$ cm^{-1} of the band edge [12]. Therefore, we hoped to see indications of excitation of these states in the contact electromodulated spectrum at energies near 2Δ. Note that, for this sample, the aperture (160 mm) is close in size to the width of the contact region.

Unfortunately, the value for the gap in blue bronze is uncertain. 2Δ has been estimated at 800 cm^{-1} from transport [18] and magnetic [27] properties, 1050 cm^{-1} from tunneling spectroscopy [28], and 1 400 cm^{-1} from a fit of the infrared spectrum [29]. In view of this uncertainty, we compare the contact and bulk electromodulated spectra over the entire spectral range available to us.

As seen in Figure 2, the two spectra are identical. (The difference in the spectra near 1 000 cm^{-1} in Figure 2d is probably due to an alignment error. It was not observed for an earlier sample [23]. Unfortunately, sample A broke before we could recheck this spectral region.) Except near absorption peaks, where the signal is very small,

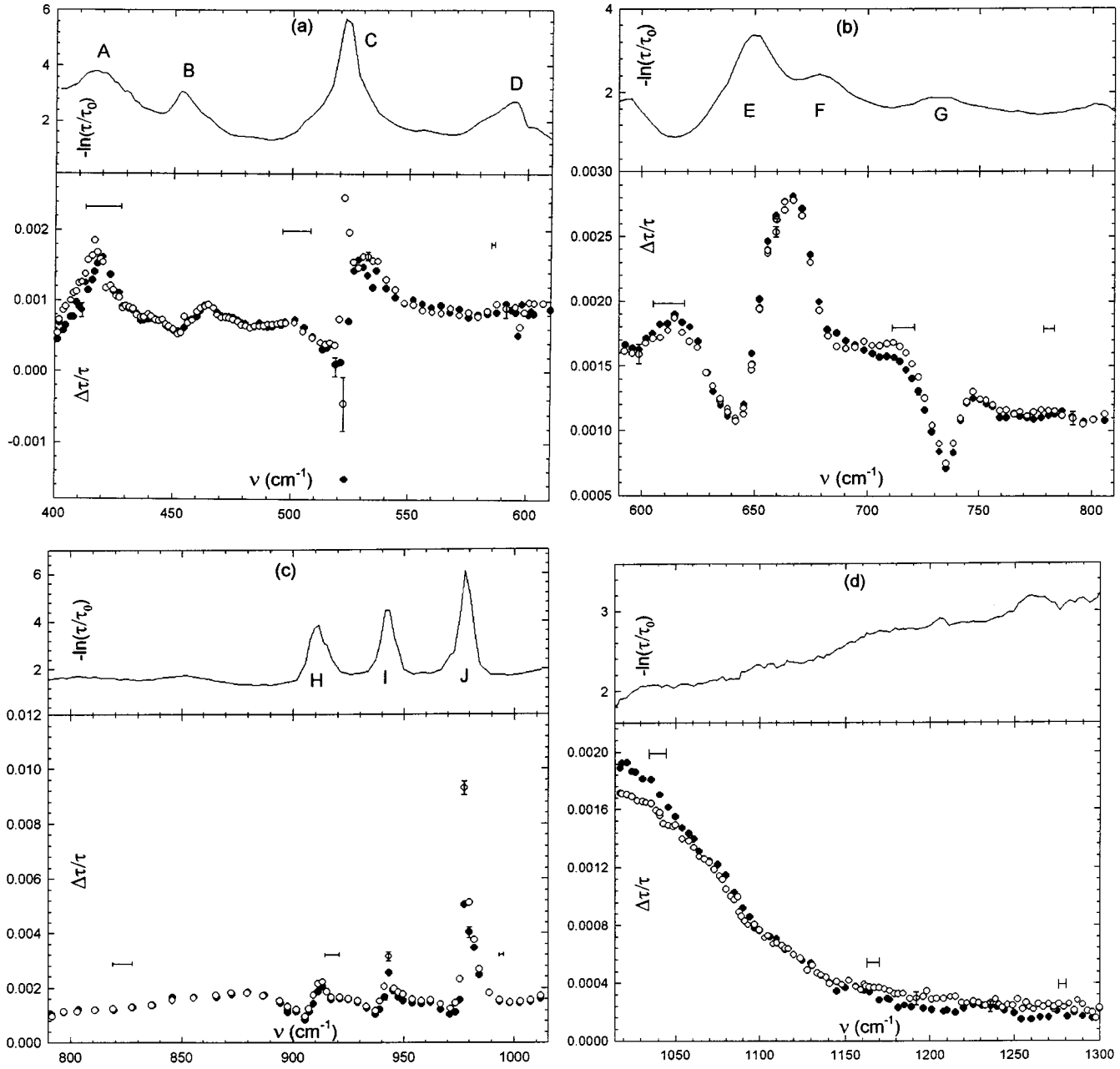

Fig. 2. The optical density and electromodulated transmission spectra of sample A at $T = 82$ K. Note that the scales are different for each panel (a-d), each taken with a different laser. For $\Delta\tau/\tau$, the solid symbols show the spectra taken with bipolar square wave voltages, $\pm V_{\rm T}$, and the open symbols show the spectra (multiplied by $N \approx 2.45$) taken with unipolar square wave voltages, $+3.2V_{\rm T}$. The letters A-J indicate phonon lines discussed in the text. Representative error bars indicating the spectral resolution and noise are shown. The scale factor $\tau_0 \approx 1$.

$\delta(\Delta\tau/\tau) \equiv |\Delta\tau/\tau$ (contact) $-(1/N)\ \Delta\tau/\tau$ (bulk) $| < 4 \times 10^{-5}$. We assume $\delta(\Delta\tau/\tau) \approx d\delta(\Delta\alpha) \approx d\,n\sigma\gamma/\Gamma$, where n, σ, and Γ are the average density, cross-section, and spectral bandwidth of the soliton states, and γ is the bandwidth of the laser, which varied due to its multimode operation. Taking $d = 3.5$ μm and $\gamma \approx 10$ cm^{-1}, we find $n\sigma/\Gamma < 10^{-10}$ (Å cm^{-1})$^{-1}$.

It is expected that $\Gamma \approx kT_{\rm c}$ [12] and $\sigma = \xi_{\|}/\xi_{\perp} \approx 100$ Å^2 [30], where $\xi_{\|}$ and $\xi_{\perp}$ are the CDW amplitude coherence lengths parallel and perpendicular to the conducting chains. If so, $n < 10^{14}$ cm^{-3}; *i.e.* there is an optically excitable intragap state on less than 1% of the chains in the contact region.

On the other hand, we expect 2π solitons to be injected at the current contact at a rate $\mathrm{d}n/\mathrm{d}t = J_{\rm CDW}/(2eL)$, where L is the width of the contact region ($\approx$ aperture width) and $J_{\rm CDW}$ ($= 1.6$ A/cm^2) is the CDW current density [1,14]. If the solitons have a lifetime t_0, then

$n \approx 5 \times 10^{20} t_0$ cm^{-3} s^{-1} in the contact region, and $\sigma t_0/\Gamma < 2 \times 10^{-7}$ Å^2 s/cm^{-1}.

Applying both the value of dn/dt and the "expected" soliton values of σ and Γ, we find that $t_0 < 0.3$ μs. This should be compared with the "narrow band noise" period $\lambda/v \approx 30$ μs [1,31] (where λ and v are the wavelength and sliding velocity of the CDW), which is the characteristic time with which dislocation lines move across the sample. Hence our results suggest that intragap excitations, created by current injection, can be optically excited for less than 1% of their total "lifetime" in the crystal. However, a few points should be noted. i) Our estimate of the optical cross-section [30] is really appropriate for light polarized parallel to the chains, whereas the light was polarized transversely in our experiments. ii) Our estimate of the cross-section is also appropriate for isolated solitons, and not necessarily for extended defects. iii) In one model of midgap excitations, their energies oscillate throughout the gap, with frequency v/λ [13]. iv) While our spectral range covers most estimates of the gap, it does not reach the value (1 400 cm^{-1}) estimated from fitting the IR conductivity to a fluctuation model [29].

In fact, we were hoping that the electrooptic effect could also be used to determine the gap. Because of large one-dimensional fluctuations, 2Δ should be identified as a cross-over energy rather than a sharp absorption edge [32]. For photon energies below the gap, the increase in transmission at the positive contact is associated with a decrease in electron density, and so a decrease in intraband absorption. There should be a corresponding increase in interband absorption for energies greater than the gap. (Opposite sign changes occur at the negative contact.) Hence we expected to observe a change in sign of the electromodulated signal at an energy near the gap edge; in fact, we had previously observed a weak inverted signal for $\nu > 1\,500$ cm^{-1} using a broadband light source [22]. However, Figure 2d shows that this inversion has not yet occurred at 1 300 cm^{-1}, the maximum frequency of our lasers. Nonetheless, the steep decrease in $\Delta\tau/\tau$ for energies above 1 000 cm^{-1}, saturating in the plateau above 1 150 cm^{-1}, suggests that the latter energy might be close to 2Δ.

4 Changes in phonon spectra caused by CDW polarization

As shown in Figure 2, the bulk and contact electromodulated spectra are identical up to a scale factor. Similarly, spectra taken at different voltages are also identical. Therefore, at a given temperature, the spectrum does not depend on CDW velocity (*i.e.* $\partial\phi/\partial t$ [1]), and all features have approximately the same ($\approx$ linear) dependence on the CDW polarization ($\partial\phi/\partial x$): $\Delta\tau/\tau(x, V, \nu) \approx S(\nu)\partial\phi/\partial x\ (x, V)$.

In the spectral region 450-670 cm^{-1}, the electromodulated spectrum is similar to the one we reported earlier, measured with a broadband light source [16]. In that study, we showed that the changes in transmission caused by an electric field were similar to those caused by a change in temperature (with voltage effectively cooling and warming the positive and negative contacts, respectively) and suggested that the electromodulated changes arise primarily through the change in $n_{\rm qp}$ accompanying CDW polarization. However, because of the strong absorption, we could not determine $\Delta\tau/\tau$ near the phonon peaks at 520 and 650 cm^{-1}. In the present study, we can resolve how the individual phonons are affected by the CDW polarization. Three types of changes in $\Delta\tau/\tau$ are observed: "M-shaped" anomalies characteristic of a change in linewidth, (inverted) "N-shaped" anomalies characteristic of a change in frequency, and (inverted) "V-shaped" anomalies characteristic of a change in oscillator strength.

Phonon G has the clearest linewidth anomaly, although phonons B and D also appear to be of this type. Recall that, as measured with the lock-in amplifier, $\Delta\tau/\tau$ is the relative change in transmission between when the contact is positive and when it is negative. The fact that $\Delta\tau/\tau$ decreases in the center of the absorption line indicates that the linewidth decreases (increases) at the positive (negative) contact. Such changes are readily understood in terms of the changes in quasiparticle density; since $n_{\rm qp}$ decreases at the positive contact, phonon damping by quasiparticle scattering also decreases, and the phonon line sharpens. Comparing the $\Delta\tau/\tau$ ($\approx -d\Delta\alpha$) and optical density ($\approx d\alpha$) spectra, we find that the width of phonon G changes by ≈ 0.03 cm^{-1} for the bulk polarization at $V_{\rm T}$. (We previously found a similar field dependent change in linewidth for a Raman mode at 480 cm^{-1}, corresponding to effective changes in temperature at the contacts of $\approx \pm 1$ K [16].) The changes in linewidths of phonons B and D are a few times smaller than this.

Phonon A appears to be the only one with an oscillator strength change. With bulk polarization, its amplitude changes by ≈ 0.07%, decreasing at the positive contact and increasing at the negative. At present, we have no explanation for these changes. While phonons can gain considerable oscillator strength from the presence of a CDW by forming a "phase-phonon" [26,33,34], these are generally polarized parallel to the conducting chain and the 420 cm^{-1} mode has not been observed to change significantly upon cooling through $T_{\rm c}$ [26].

Phonons C, E, H, I, and J have predominantly frequency shift anomalies, although asymmetries in their lineshapes (*e.g.* for J) are presumably because their linewidths and/or oscillator strengths change as well. (No electromodulated change in phonon F is detected, possibly because its changes are overwhelmed by those in E.) Comparison of the $\Delta\tau/\tau$ and optical density spectra indicate that, for bulk polarization, the frequency shifts vary from $\approx 5 \times 10^{-3}$ cm^{-1} (for I) to 3×10^{-2} cm^{-1} (for E). (For C, the electromodulated signal has the appearance of two superimposed inverted "N's", one much sharper than the other, suggesting that there are two modes at this energy, consistent with its σ_1 lineshape [26].)

In all cases, the "inverted-N" shape of the anomalies indicates that the frequencies decrease (increase) at the positive (negative) contact. This is the opposite

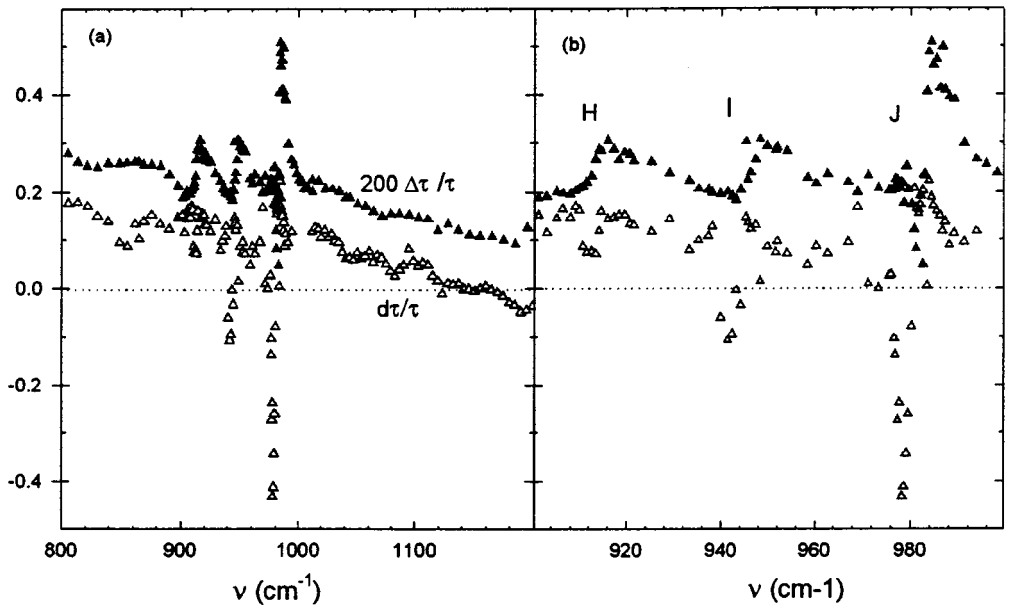

Fig. 3. (a) Thermal modulated transmission, $d\tau/\tau \equiv [\tau(T-4K)-\tau(T+4K)]/\tau(T)$, and electromodulated transmission ($\Delta\tau/\tau$) spectra of sample B at $T = 102$ K. (b) Enlargement of the spectral region near phonons H, I, and J [22].

of what would be expected from quasiparticle damping, and so these changes in transmission cannot be similar to temperature dependent changes. Figure 3 compares the bipolar spectrum (between 800 and 1 200 cm^{-1}) of $\Delta\tau/\tau$ for sample B at $T = 102$ K with the relative change in transmission with change in temperature, $d\tau/\tau \equiv [\tau(T-4K)-\tau(T+4K)]/\tau(T)$. (The bipolar spectrum was measured with $V = \pm 3\,V_T$, so in principle includes effects of both contact and bulk polarization, but the contact contribution in this sample was very small [22].) In contrast to the inverted "N-shaped" anomalies observed in the $\Delta\tau/\tau$ spectra for phonons H, I, and J, the anomalies in the $d\tau/\tau$ spectra are "M-shaped", as expected for thermal broadening. Also note that the absorption edge is much sharper in the thermal modulated spectrum than in the electromodulated spectrum. In fact, $d\tau/\tau$ changes sign at 1 100 cm^{-1}. A cross-over in the temperature dependence of σ_1 at this energy was also found by Degiorgi, *et al.* [29], and associated with the broadening of the CDW gap due to thermal and quantum fluctuations. The large size of the thermally modulated signal as compared to the electromodulated signal is due to the relatively strong temperature dependence of the absorption edge near 100 K [29].

We previously suggested [22,23] that the frequency shifts of the phonons in the electromodulated spectra may be due to resonant mixing of the phonons with states in the gap due to these fluctuations [32]. In this case, the phonon anomalies should only be weakly temperature dependent, reflecting the weak temperature dependence of the "disorder" creating these intragap states [29]; most of the disorder is a consequence of quasi-one dimensional quantum fluctuations. Alternatively, the phonons may be interacting with virtual electron-hole excitations across the CDW gap, decreasing the phonon energies (assuming $\nu < 2\Delta$). When the quasiparticle density decreases at the positive contact, it will increase the strength of this mixing, further decreasing the phonon energy, as observed. In this case, the frequency shifts should be approximately activated, although the temperature dependence of the Fermi energy may weaken this temperature dependence somewhat.

The electromodulated spectra (580 to 1 115 cm^{-1}) measured for sample C at a few temperatures are shown in Figure 4. Spectra were taken with bipolar, $V = \pm V_T(T)$, modulation, and so correspond to the bulk polarization. It is seen that the frequency shifts of modes E, H, I, and J, proportional to their peak-peak $\Delta\tau/\tau$ variations, decrease considerably with decreasing temperature, although not as strongly as the overall $\Delta\tau/\tau$ signal. In fact, as shown in the inset, the frequency shifts have activation energy ≈ 150 K, approximately half that of the dc conductivity. (Note that the conductivity activation energy is smaller than its value above 100 K [14].) It may be that the phonon frequency shifts arise from more than one mechanism, with different temperature dependences, but, as emphasized above, all are approximately proportional to the CDW strain.

In summary, we have examined electromodulated infrared transmission spectra of blue bronze in detail. The spectra associated with charge injection at current contacts is identical to that associated with bulk polarization of the CDW, and there is no indication of new intragap states associated with the injection. Phonon lines are affected in different ways by CDW polarization. Some phonons broaden, as would be expected due to the changes in quasiparticle density that accompany polarization. However other phonons exhibit changes in oscillator strength or frequency, which are more difficult to understand.

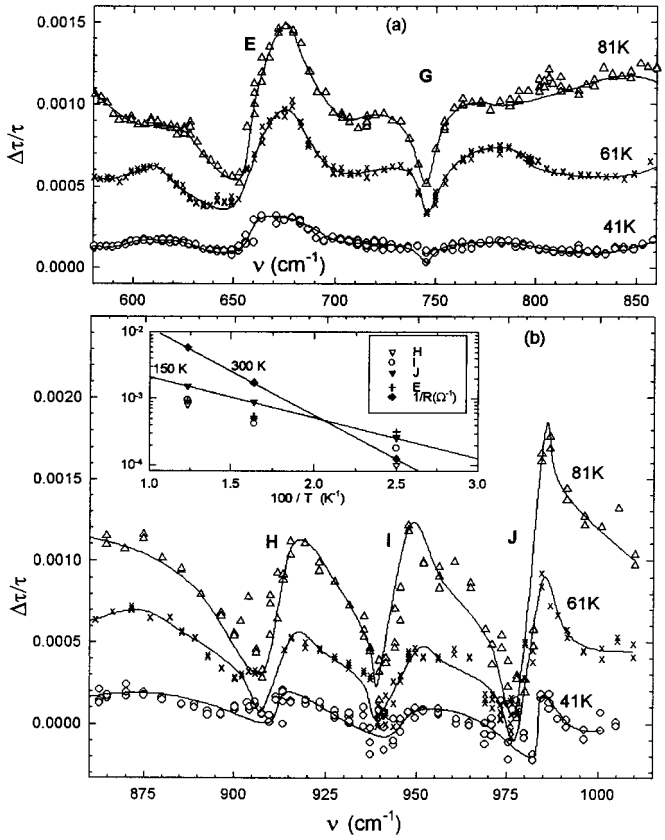

Fig. 4. Electromodulated transmission spectra of sample C at 3 temperatures: (a) 580–860 cm^{-1}; (b) 860–1 115 cm^{-1}. E, G, H, I, J denote phonon lines discussed in the text. The curves are guides to the eye. Inset: Temperature dependence of the crystal's dc resistance (R) and the peak to peak modulation in $\Delta\tau/\tau$ for phonons E, H, I, and J. The reference lines have slopes of 300 K and 150 K, as indicated.

We thank R.E. Thorne and A. Zettl for providing crystals, and S. Artemenko, S. Brazovski, and G. Murthy for helpful discussions. This research was supported by the US National Science Foundation, Grant #DMR-9731257.

References

1. G. Gruner, Rev. Mod. Phys. **60**, 1129 (1988).
2. J.C. Gill, Solid State Commun. **44**, 1041 (1982).
3. K. Maki, Physica B **143**, 59 (1986).
4. D. Feinberg, J. Friedel, *Low-Dimensional Electronic Properties of Molybdenum Bronzes and Oxides*, edited by C. Schlenker (Kluwer, Dordrecht, 1989), p. 407.
5. J.C. Gill, J. Phys. Condens. Matter **1**, 6649 (1989); J. Phys. IV France **9**, Pr10-97 (1999).
6. S. Brazovskii, N. Kirova, Synth. Met. **103**, 2589 (1999); J. Phys. IV France **9**, Pr10-139 (1999).
7. T.L. Adelman, *et al.*, Phys. Rev. B **53**, 1833 (1996).
8. S.G. Lemay, *et al.*, Phys. Rev. B **57**, 12781 (1998).
9. H. Requardt, *et al.*, Phys. Rev. Lett. **80**, 5631 (1998); J. Phys. IV France **9**, Pr10-133 (1999).
10. M.E. Itkis, B.M. Emerling, J.W. Brill, Phys. Rev. B **52**, R11545 (1995).
11. M.E. Itkis, B.M. Emerling, J.W. Brill, Synth. Met. **86**, 1959 (1997).
12. S. Brazovskii, S. Matveenko, J. Phys. I France **1**, 269, 1173 (1991).
13. S.N. Artemenko, A.F. Volkov, A.N. Kruglov, Sov. Phys. JETP **64**, 906 (1987).
14. C. Schlenker, *Low-Dimensional Electronic Properties of Molybdenum Bronzes and Oxides*, edited by C. Schlenker (Kluwer, Dordrecht, 1989), p. 159.
15. M.E. Itkis, J.W. Brill, Phys. Rev. Lett. **72**, 2049 (1994).
16. M.E. Itkis, B.M. Emerling, J.W. Brill, Phys. Rev. B **56**, 6506 (1997).
17. M. Cardona, *Modulation Spectroscopy* (Academic, New York, 1969).
18. L. Forro, *et al.*, Phys. Rev. B **34**, 9047 (1986).
19. J. Chaussy, *et al.*, Solid State Commun. **20**, 759 (1976).
20. J.C. Gill, Solid State Commun. **39**, 1203 (1981); R.M. Fleming, L.F. Schneemeyer, Phys. Rev. B **28**, 6996 (1983); L. Mihaly, A. Janossy, Phys. Rev. B **30**, 3530 (1984).
21. Laser Analytics, Inc., Wilmington, Massachussetts, USA.
22. B.M. Emerling, M.E. Itkis, J.W. Brill, Synth. Met. **103**, 2598 (1999).
23. B.M. Emerling, M.E. Itkis, J.W. Brill, J. Phys. IV France **9**, Pr10-125 (1999).
24. G. Travaglini, *et al.*, Solid State Commun. **37**, 599 (1981).
25. N.E. Massa, Phys. Rev. B **34**, 5943 (1986).
26. S. Jandl, *et al.*, Phys. Rev. B **40**, 12487 (1989).
27. D.C. Johnston, Phys. Rev. Lett. **52**, 2049 (1984).
28. K. Nomura, K. Ichimura, J. Vac. Sci. Technol. **A8**, 504 (1990).
29. L. Degiorgi, *et al.*, Phys. Rev. B **52**, 5603 (1995).
30. G. Minton, J.W. Brill, Phys. Rev. B **45**, 8256 (1992).
31. G. Mihaly, *et al.*, Phys. Rev. B **37**, 1047 (1988).
32. R.H. McKenzie, J.W. Wilkens, Phys. Rev. Lett. **69**, 1085 (1992).
33. M.J. Rice, Phys. Rev. Lett. **37**, 36 (1976).
34. L. Degiorgi, *et al.*, Phys. Rev. B **44**, 7808 (1991).